Numerical Prediction of Axial Strength in Square Concrete-Filled Steel Tube Columns

S K Katariya[1] Suryakant Deoli[2]

1. S K Katariya, Associate Professor, 2. M.Tech. student

Department of Civil Engineering, COT Pantnagar, Uttarakhand, India

ABSTRACT

Concrete-filled steel tube (CFST) columns are widely employed in modern structural systems due to their high axial load-carrying capacity, enhanced ductility, and efficient composite action between steel and concrete. Although extensive research has been conducted on circular CFST columns, the axial behavior of square CFST sections remains more challenging to characterize because of their non-uniform confinement and localized stress concentrations. This study presents a numerical formulation for predicting the axial strength of square CFST columns. The proposed model accounts for nonlinear material behavior and steel–concrete interaction to closely replicate the actual structural response. The numerical predictions were validated against experimental results available in the literature, demonstrating strong agreement in terms of ultimate load. The peak load ratios between experimental and numerical results were also evaluated to assess the accuracy of the developed formulation. Finally, validated stress–strain curves are provided, illustrating how closely the proposed method reproduces the experimentally observed behavior. The findings confirm that the numerical formulation offers an accurate and reliable tool for analyzing and optimizing the design of square CFST columns.

Keywords: Concrete-Filled Steel Tubes, Axial Load, Stress-Strain curve, Confined Concrete, Digitization of graphs.

I. INTRODUCTION

Concrete-filled steel tube (CFST) members are widely used in modern high-rise buildings, long-span bridges, and seismic-resistant structures due to their superior mechanical and structural performance. A CFST column consists of a hollow steel tube filled with concrete, forming a composite section that exhibits high ductility, enhanced bearing capacity, and improved resistance to external loading. The confining action provided by the steel tube restrains lateral expansion of the concrete core, thereby increasing the strength and delaying crushing failure. This confinement mechanism significantly improves the overall load-carrying capacity of the member, making CFST columns highly suitable for earthquake-resistant and high-performance structural applications.

Beyond their mechanical advantages, CFST columns also offer several practical benefits. The steel tube acts simultaneously as reinforcement and permanent formwork, reducing the need for conventional shuttering and accelerating construction. Their high energy absorption capacity, durability, and inherent fire resistance further contribute to their widespread use in structural engineering practice. The external steel tube can be fabricated in various cross-sectional shapes—such as circular, square, rectangular, or octagonal—depending on architectural and structural requirements.

Among these, square CFST columns provide additional benefits, including superior biaxial load resistance and easier beam-column connections, making them especially suitable for building frames. However, the behavior of confined concrete in square sections is more complex due to non-uniform confinement and stress concentration at the corners. In this study, the behavior of square confined concrete is investigated, and a predictive equation is developed to estimate its axial performance accurately.

2 METHODS AND MATERIAL

A comprehensive review of research articles on concrete-filled steel tube (CFST) columns was conducted, with particular emphasis on axially loaded square CFST specimens without stiffeners or additional reinforcement. Load–axial shortening and load–strain graphs from previously published studies were collected and digitized for detailed analysis. A total of 14 square CFST specimens were selected for developing the proposed predictive equation. These specimens were taken from earlier experimental investigations on square CFST columns. The study aims to formulate a single equation that directly relates the concrete stress to its corresponding strain. The proposed equation was validated by comparing the numerically generated stress–strain curves with the digitized experimental data, demonstrating the accuracy of the computational model.

2.1 Grade of concrete

The cylinder strength of concrete plays a significant role in the structural performance of square CFST columns. In the selected specimens, the cylindrical compressive strength ranged from 24.7 MPa to 106 MPa, denoted as f_c'. From the review of square CFST sections, it was evident that $f_c'$is a key parameter governing the axial strength of square CFST members. The digitized specimens used in this study possessed the following material characteristics.

2.2 Grade of Steel

The grade of steel used in the selected specimens varied between 192 MPa and 835 MPa. The stress–strain behavior of steel was adopted from the model proposed by Dalin Liu and Wie-Min Gho, which served as the basis for developing the confined concrete equation. The Young's modulus of elasticity for steel was taken as 200,000 MPa. The strain corresponding to the yield stress was determined by dividing the yield strength of the steel by its modulus of elasticity.

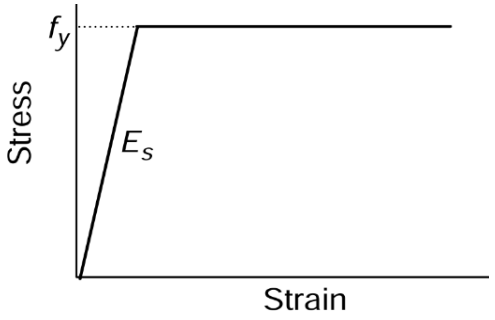

Fig. 1 Liu and Gho Model of steel

3. DEVELOPMENT OF PROPOSED EQUATION

The procedure to obtain the stress-strain curve of confined concrete of square CFST is given below:

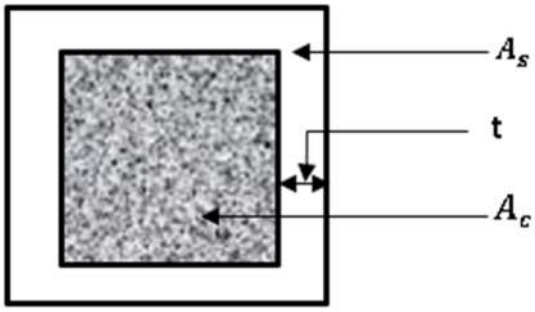

Fig. 2. Cross section of square CFST column

$$P_{exp} = P_s + P_c \quad (1)$$

$$P_s = \sigma_s \times A_s \quad (2)$$

$$A_s = A_t - A_c \quad (3)$$

$$A_t = B \times B \quad (4)$$

$$A_c = (B - 2 \times t)^2 \quad (5)$$

$$\sigma_c = \frac{P_c}{A_c} \quad (6)$$

$$\sigma_c = \frac{P_{exp} - P_s}{A_c} \quad (7)$$

The axial load carried by a square CFST specimen can be expressed as the sum of the load resisted by the steel tube and the load resisted by the confined concrete. Here, P_{exp}denotes the experimentally measured axial load of the square CFST specimen, $P_s$is the load carried by the steel tube, and $P_c$is the load carried by the concrete core. The steel stress is represented by σ_s, with $A_s$denoting the cross-sectional area of steel. The total cross-sectional area of the CFST member is A_t, while $A_c$represents the area of the concrete core. The specimen width is denoted by B, and $t$is the thickness of the outer steel tube. The concrete stress in the CFST column is represented by σ_c.

Using these parameters, the confined concrete stress–strain curve was obtained. For this purpose, the CFST specimens reported by Liang et al. were utilized, and their material properties were compiled along with the digitized properties of the selected specimens for further analysis.

Table 1. Material and geometric property of digitized specimens

Reference	Specimen	B×B (mm×mm)	t (mm)	$\frac{D}{t}$	f'_c (MPa)	f_y (MPa)
Liang *et al.* (2006)	S1	127×127	3.15	55.45	30.5	356
	S2	127×127	4.34	29.26	26.0	357
	S3	127×127	4.55	27.91	23.85	322
Ouyang and Kwan (2018)	CR4-A-4-1	148×148	4.38	33.78	40.5	262
	CR8-A-8	119×119	6.47	18.39	77	835
	CR8-C-8	175×175	6.47	27.04	77	835
	A1	120×120	5.8	20.68	83	300
	A2	120×120	5.8	20.68	106	300
Dalin Liu (2004)	R7-1	106×106	4	26.4	89	495
	R1-1	120×120	4	30	60	495
Ne Shanmugam (2006)	HS7	126×126	2.14	40	50	282
Qing Quan Liang (2009)	I-A	100×100	2.29	43.7	38.4	197
	II-A	100×100	2.20	45.5	25.7	345
	III-B	100×100	2.99	33.4	24.7	293

Table 2. Material and geometric property of Liang et all specimens

Ref	B×B (mm×mm)	t (mm)	D/t	f_c' (MPa)	f_y (MPa)	Specimen Name
Liang *et al.* (2009)	100 ×100	2.29	43.7	38.4	197	I-A
	100 ×100	2.20	45.5	25.7	345	II-B
	100 ×100	2.99	33.4	24.7	293	III-B
	100 ×100	4.25	23.5	23.8	289	IV-A

A regression analysis was carried out for the data obtained through calculation of confined stress obtained by equation (7). The result obtained through this analysis is provided below:

$$y = \frac{a+bx}{1+cx+dx^2} \quad (9)$$

Where x, y are the strain and stress of confined concrete the value of a = -0.75954, b=3.11465067 × 10^4, c= 4.93404369 ×10^2, d= 9.4706967 ×10^4

The equation was made through Liang et all specimen by taking the average compressive strength of concrete to be 28.18 MPa. This equation was subsequently simplified to incorporate a modification that accounts for variations in the compressive strength of concrete.

The value of coefficient of a is -.07597 which is taken to be 0, then the equation becomes

$$y = \frac{ax}{1+bx+cx^2} \quad (10)$$

Where a=3.11465067 × 10^4, b=4.93404369 ×10^2 and c= 9.4706967 ×10^4

The above given equation is for 28.15 MPa compressive strength of concrete to account for different cylinder strength of concrete f_c' the equation is modified as follows:

$$y = \frac{\frac{31146.51}{28}x}{1+493.4044x+94706.968x^2} \times f_c' \quad (11)$$

Final equation after all the modification is

$$y = \frac{1100x}{1+500x+95000x^2} \times f_c' \quad (12)$$

Where y is the stress of confined concrete and x is strain corresponding to it.

Using Equation (12), the confined concrete stress in a square CFST specimen can be determined. Once the concrete area for each specimen is calculated, the corresponding load carried by the concrete core can be obtained. Similarly, the load carried by the steel tube is computed and added to the concrete load at the same strain level, yielding the complete load–strain response of the square CFST column. The numerically generated curves for all 14 specimens were then compared with their experimentally digitized counterparts to evaluate the accuracy and reliability of the proposed equation. Fig. 3 shows the validation of experimental stress-strain behaviour 28 MPa strength concrete with stress-strain behaviour obtained by proposed model for the same strength concrete.

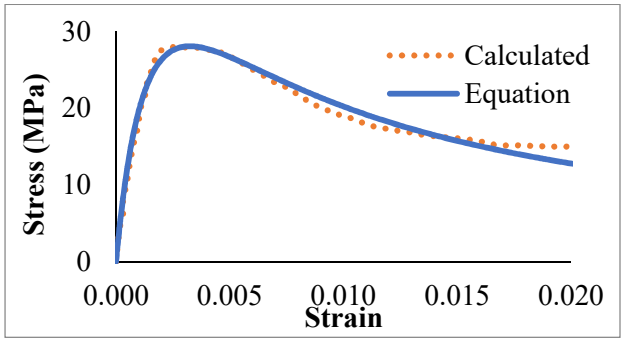

Fig. 3. Comparison of experimental curve with proposed equation curve for 28MPa confined concrete

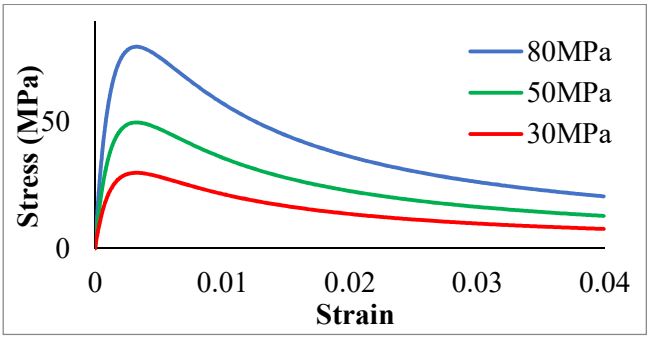

Fig. 4. Stress-strain curve of confined concrete by proposed equation for different compressive strength

Table 3. Peak ratios and material property of validated specimens

Reference	Specimen Names	B×B (mm×mm)	t (mm)	$\frac{D}{t}$	f_c' (MPa)	f_y (MPa)	P_{exp} (kN)	P_{comp} (kN)	$\frac{P_{exp}}{P_{comp}}$
Liang *et al.* (2006)	S1	127×127	3.15	55.45	30.5	356	900	997.97	0.917
	S2	127×127	4.34	29.26	26.0	357	1098.20	1122.65	0.978
	S3	127×127	4.55	27.91	23.85	322	1106.30	1047.80	1.056

Y. Ouyang & A.K.H. Kwan (2018)	CR4-A-4-1	148×148	4.38	33.78	40.5	262	1412.52	1441.18	0.990
	CR8-A-8	119×119	6.47	18.39	77	835	3313.52	3261.95	1.017
	CR8-C-8	175×175	6.47	27.04	77	835	5353.03	5621.26	0.953
	A1	120×120	5.80	20.68	83	300	1670.23	1742.83	0.958
	A2	120×120	5.80	20.68	106	300	1922.27	2035.43	0.944
Dalin Liu (2004)	R7-1	106×106	4.00	26.4	89	495	1715.26	1659.15	1.034
	R1-1	120×120	4.00	30.00	60	495	1696.58	1668.00	1.056
Shanmugam (2006)	HS7	126×126	2.14	40.00	50	282	1704.70	1654.98	1.030
Qing Quan Liang (2009)	I-A	100×100	2.29	43.70	38.4	197	509.467	520.077	0.980
	II-B	100×100	2.20	45.50	25.7	345	523.664	530.862	0.986
	III-B	100×100	2.99	33.40	24.7	293	509.484	557.337	0.914

The validation is carried out for all the 14 square CFST specimens given below:

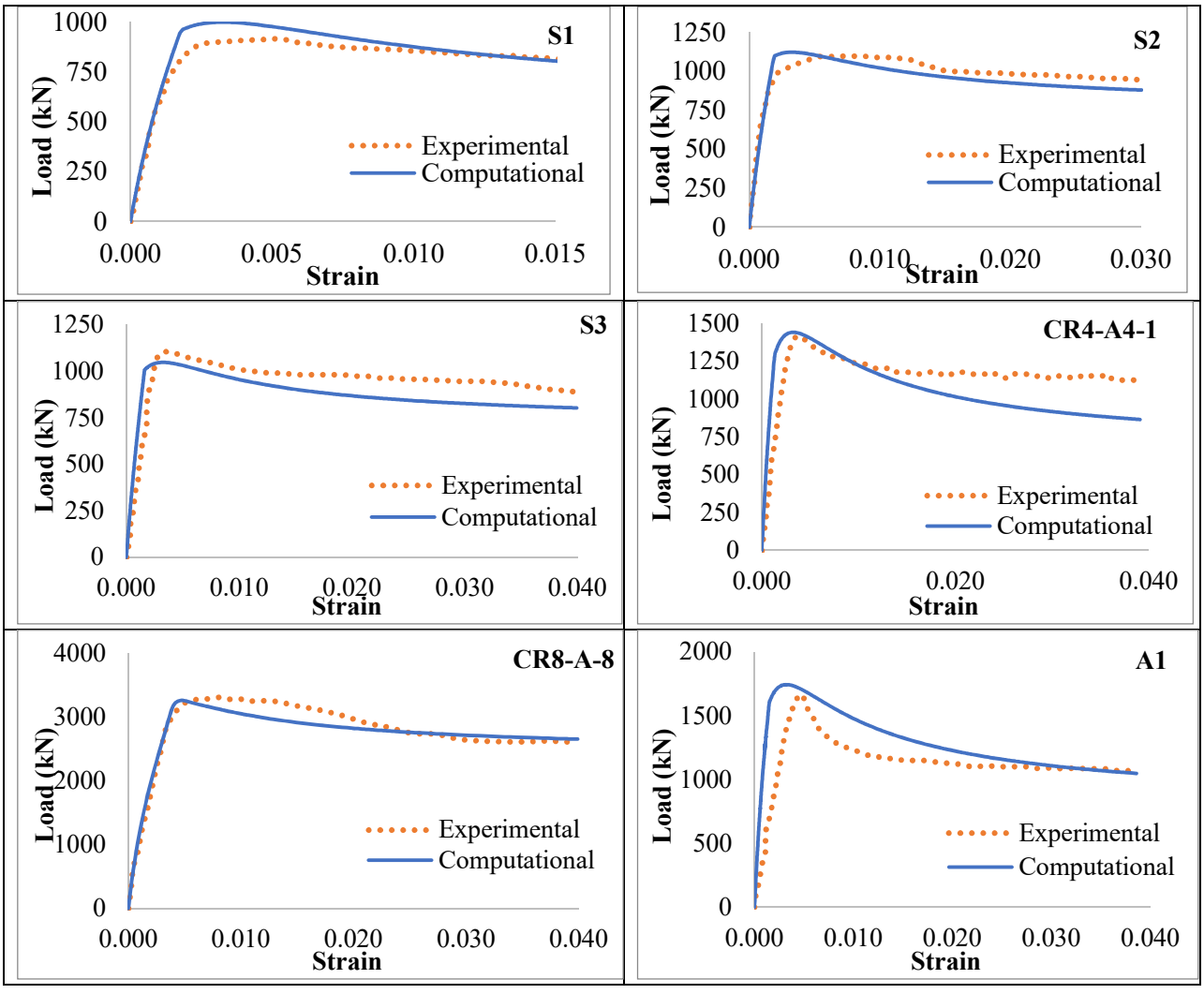

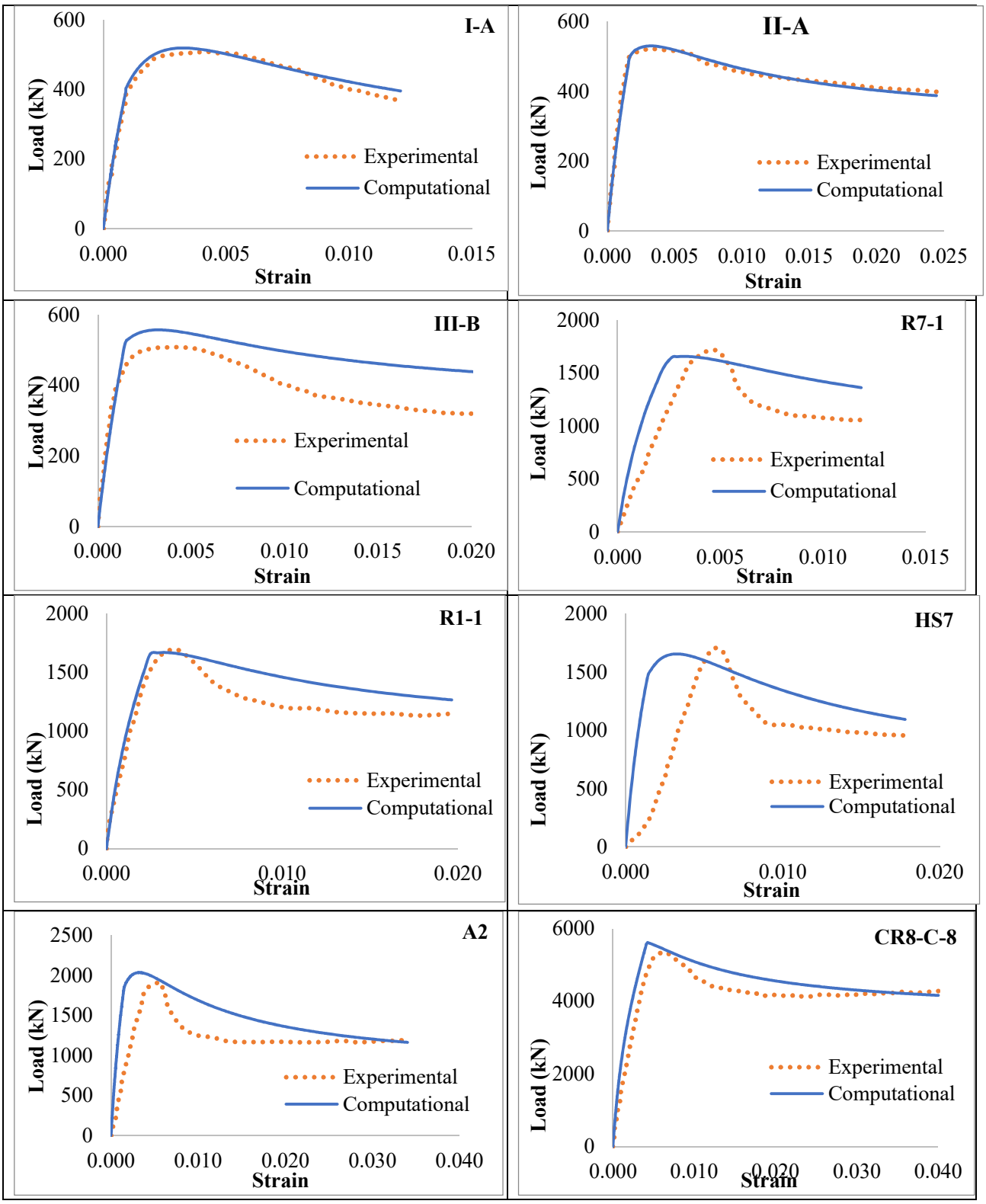

Figs. 5. Validation of load-strain behaviour of specimens with load -strain behaviour obtained by proposed model.

4 RESULTS

The axial compression behaviour of the square CFST columns for all specimens is presented in Fig. 5. The material properties, geometric details, and sources of the 14 specimens are summarised in Tables 1–3. The load–strain responses of these specimens were validated by comparing the experimental curves with those predicted by the proposed equation. These comparison show a good agreement between experimental behavior and results obtain using proposed model.

5 CONCLUSIONS

1. The equation developed for the confined square concrete obtained through regression analysis of data is

$$y = \frac{1100x}{1+500x+95000x^2} \times f_c'$$

The nonlinear stress–strain behavior of confined concrete is accurately represented by the proposed equation, which captures both the initial elastic response and the subsequent plastic deformation. The denominator term $(1 + 500x + 95{,}000x^2)$introduces the curvature necessary to transition from linear elasticity to post-peak softening behavior.

1. The $1100x$ term in the numerator reflects the rapid increase in stress at low strain levels, while the quadratic term $95{,}000x^2$governs the post-peak response at higher strains.
2. A novel analytical method has been developed for predicting the axial behavior of square CFST columns.
3. At a compressive strength of 30 MPa, the stress–strain curve initially follows a linear path before gradually transitioning into a nonlinear regime, signifying elastic behavior followed by yielding.
4. For concrete strengths of 50 MPa and 80 MPa, the curves become steeper, demonstrating higher stiffness and greater resistance to deformation. This confirms that higher-grade concrete offers enhanced strength and reduced susceptibility to strain.
5. The curves diverge significantly at strain levels beyond 0.002, highlighting the plastic behavior of confined concrete and the influence of compressive strength on post-yield response.
6. The experimental and computational curves exhibit similar ascending trends, indicating that the developed model successfully captures the material behavior of square CFST columns.
7. The ratio of computational peak load to experimental peak load is close to unity, with an average value of 1.03. This confirms that the proposed equation provides an accurate prediction of the axial capacity of square CFST columns.

REFERENCE

[1] Liang, Q. Q., Uy, B., & Liew, J. Y. R. (2006). Nonlinear analysis of concrete-filled thin-walled steel box columns with local buckling effects. *Journal of Constructional Steel Research, 62*(6), 581–591. https://doi.org/10.1016/j.jcsr.2005.09.007

[2] Liang, Q. Q., & Fragomeni, S. (2009). Nonlinear analysis of circular concrete-filled steel tubular short columns under axial loading. *Journal of Constructional Steel Research, 65*(12), 2186–2196. https://doi.org/10.1016/j.jcsr.2009.06.015

[3] Liu, D., Gho, W.-M., & Yuan, J. (2003). Ultimate capacity of high-strength rectangular concrete-filled steel hollow section stub columns. *Journal of Constructional Steel Research, 59*(12), 1499–1515. https://doi.org/10.1016/S0143-974X(03)00106-8

[4] Liu, D., & Gho, W.-M. (2005). Axial load behaviour of high-strength rectangular concrete-filled steel tubular stub columns. *Thin-Walled Structures, 43*(8), 1131–1142. https://doi.org/10.1016/j.tws.2005.03.007

[5] Ouyang, Y., & Kwan, A. K. H. (2018). Finite element analysis of square concrete-filled steel tube (CFST) columns under axial compressive load. *Engineering Structures, 156*, 443–459. https://doi.org/10.1016/j.engstruct.2017.11.055

[6] Shanmugam, N. E., & Lakshmi, B. (2001). State of the art report on steel–concrete composite columns. *Journal of Constructional Steel Research, 57*(10), 1041–1080. https://doi.org/10.1016/S0143-974X(01)00021-9